BRIEF COMMUNICATION
https://doi.org/10.1038/s41558-022-01282-z

nature climate change



OPEN

# Increased ENSO sea surface temperature variability under four IPCC emission scenarios

Wenju Cai[1,2]✉, Benjamin Ng[2], Guojian Wang[1,2], Agus Santoso[2,3], Lixin Wu[1]✉ and Kai Yang[4]

**Sea surface temperature (SST) variability of El Niño–Southern Oscillation (ENSO) underpins its global impact, and its future change is a long-standing science issue. In its sixth assessment, the IPCC reports no systematic change in ENSO SST variability under any emission scenarios considered. However, comparison between the 20th and 21st century shows a robust increase in century-long ENSO SST variability under four IPCC plausible emission scenarios.**

The summary for policymakers of the IPCC Sixth Assessment Report[1] (AR6) has reaffirmed that it is "very likely that the ENSO rainfall variability is projected to be amplified by the second half of the 21st century" in most emission scenarios, consistent with findings by previous studies of a stronger rainfall response to ENSO SST variability even if ENSO SST variability itself does not change[2–4]. This assessment is reinforced in Chapter 4 of AR6 that "it is very likely that ENSO rainfall variability, used for defining extreme El Niños and La Niñas, will increase significantly, regardless of amplitude changes in ENSO SST variability, by the second half of the 21st century" in most emission scenarios. However, the AR6 report further states that "there is no model consensus for a systematic change in intensity of ENSO sea surface temperature (SST) variability over the 21st century in any of the SSP scenarios assessed (medium confidence)," which we find does not reflect findings of the latest research.

The IPCC AR6 statement on ENSO SST variability is contrary to studies[5–7] based on climate models participating in the sixth phase of the Coupled Model Intercomparison Project[8] (CMIP6). There was a lack of inter-model consensus among available models that participated in the previous instalments of CMIP5, unless model selection was applied on the basis of the realism of the simulated ENSO[9,10]. However, CMIP6 models exhibit a notably higher inter-model consensus than CMIP5 models under a high emission scenario[7]. Because ENSO SST variability underpins consequential ENSO-related climate variability and climate extremes within and outside the Pacific[6,11,12], how ENSO SST variability might respond to greenhouse warming is a fundamental issue in climate change science[7,9,13], with critical societal ramifications. As such, the cause for the discrepancy needs clarification.

The AR6 assessment on ENSO change is based on evolution of ENSO SST variability in the central-to-eastern equatorial Pacific (Niño3.4 area: 5° N–5° S, 170° W–120° W) over 30-year periods, normalized by averaged variability over the 20-year current climate of 1995–2014 (Fig. 4.10a of Chapter 4, IPCC Report[1]) simulated by CMIP6 models under various emission scenarios. However, sampling ENSO SST variability over relatively short 30-year running periods would be subject to a strong influence from decadal climate fluctuations such that stochastic noise and butterfly effect can obscure the impact of greenhouse forcing[14–16]. Even on centennial timescales, ENSO variability is influenced by internal climate fluctuations[17]. Here we show that, contrary to the AR6 assessment, ENSO SST variability is stronger in the 21st century than in the 20th century in four plausible emission scenarios considered in the IPCC AR6.

We construct monthly evolution of SST anomalies covering the period 1900–2099, under four shared socioeconomic pathways (SSP)[8] in available CMIP6 models (39 models under SSP126, 42 under SSP245, 38 under SSP370, and 43 under SSP585) (Supplementary Table 1) (see 'CMIP6 models' in Methods). One experiment from each model is used as in the IPCC AR6. The SST anomalies are then quadratically detrended and averaged over traditional regions of ENSO SST indices. These include Niño3 (5° N–5° S, 150° W–90° W), Niño4 (5° N–5° S, 160° E–150° W) and Niño3.4, used to depict Eastern Pacific ENSO variability, Central Pacific ENSO variability, and their combined variability, respectively.

Under SSP585, a 'high emissions' scenario in the 21st century (2000–2099) sees greater Niño3.4 variability than in the 20th century (1900–1999) in a total of 38 out of 43 (88.4%) models (Fig. 1a). The multi-model ensemble mean increase (16.1%) is statistically significant according to a Bootstrap method[18] (see 'Bootstrap test' in Methods and Extended Data Fig. 1). A similar increase (15.7%) is obtained when inter-model differences in representing ENSO amplitude are removed (Extended Data Fig. 2). In terms of Niño3 and Niño4 SST variability, the level of inter-model consensus is also strong, both reaching 81.4%, consistent with recent studies[5–7]. Using more sophisticated indices leads to an even stronger consensus[7].

Inter-model consensus is seen in all four SSP emission scenarios (Extended Data Figs. 3, 4 and 5), ranging between 78.6–88.4% for Niño3.4, 76.2–81.6% for Niño3, and 73.8–81.4% for Niño4 across emission scenarios. In the SSP126 scenario (Fig. 1b), which represents a strong mitigation path under the Paris Agreement to limit warming to 1.5–2.0 °C relative to the pre-industrial level, a total of 34 out of 39 models (87.2%) generate an increase in Niño3.4 SST variability. The multi-model ensemble mean increase (11.7%) is statistically significant. Thus, even if the Paris Agreement target is achieved, an increase in ENSO SST variability is projected, con-

[1]Key Laboratory of Physical Oceanography–Institute for Advanced Ocean Studies, Ocean University of China and Qingdao National Laboratory for Marine Science and Technology, Qingdao, China. [2]Center for Southern Hemisphere Oceans Research (CSHOR), CSIRO Oceans and Atmosphere, Hobart, Australia. [3]Australian Research Council (ARC) Centre of Excellence for Climate Extremes, The University of New South Wales, Sydney, Australia. [4]State Key Laboratory of Numerical Modeling for Atmospheric Sciences and Geophysical Fluid Dynamics, Institute of Atmospheric Physics, Chinese Academy of Sciences, Beijing, China. ✉e-mail: Wenju.cai@csiro.au; Lxwu@ouc.edu.cn

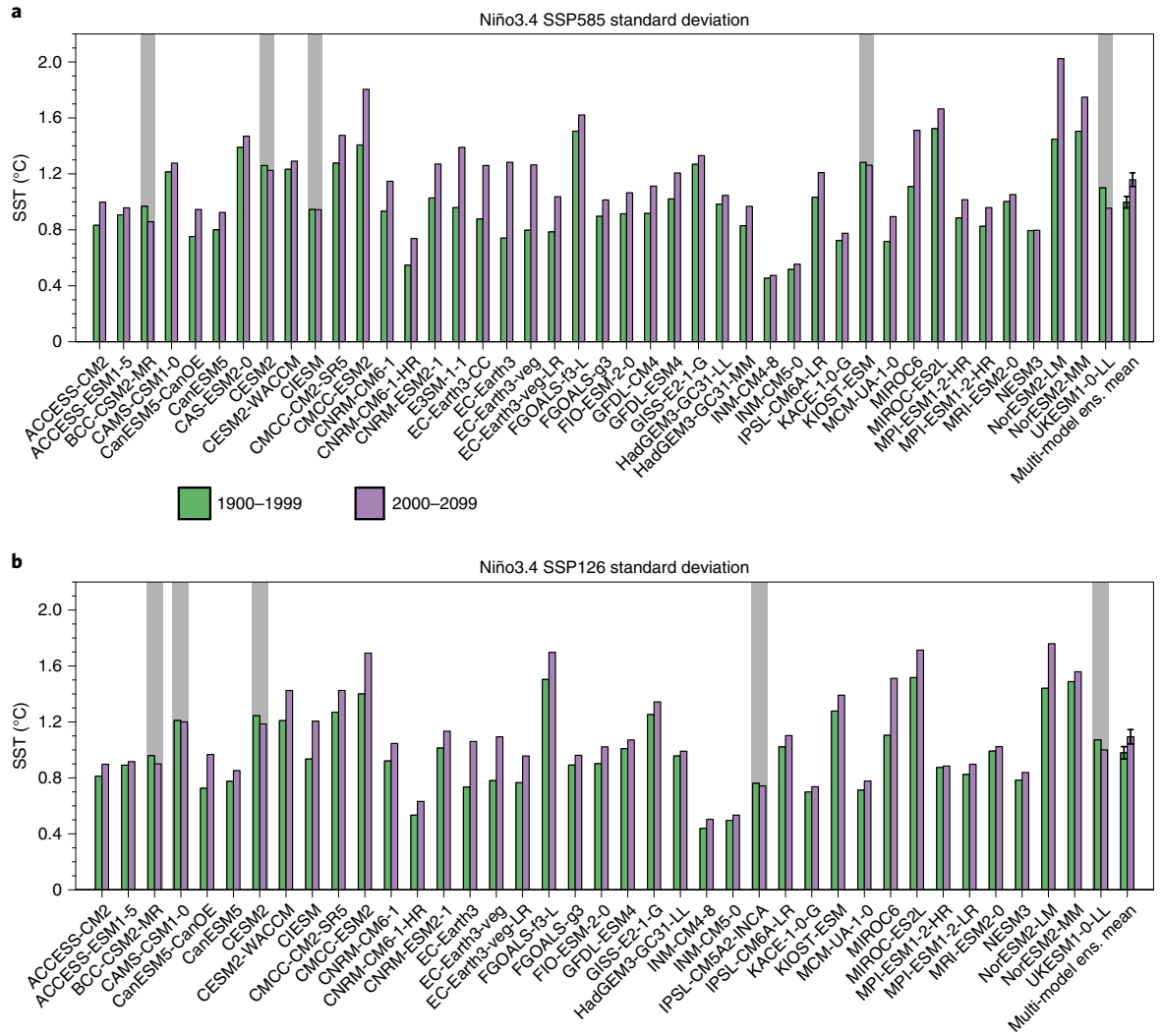


**Fig. 1 | An inter-model consensus on increased ENSO SST variability. a**,**b**, ENSO Niño3.4 SST standard deviation (in °C) over the 20th century (1900–1999, green bars) and the 21st century (2000–2099, purple bars) from 43 available CMIP6 models under the SSP585 scenario (**a**), and from 39 CMIP6 models under the SSP126 scenario (**b**), with 88.4% and 87.2% of models respectively showing an increase in ENSO variability. The grey shading indicates models which do not simulate an increase. Also shown is the multi-model ensemble mean for each period. The error bars in the multi-model mean bars are defined as the value of the standard deviation of inter-model variability in the 20th and 21st centuries, determined by a Bootstrap test (see 'Bootstrap test' in Methods). The difference in the multi-model mean is statistically significant above the 95% confidence level.

sistent with previous results in terms of ENSO rainfall variability, which show a continuous increase after global mean temperature stabilizes[4].

As mentioned above, influence from internal variability could explain the lack of inter-model consensus in the AR6[14–16]. Using statistics over another longer period, for example, 50 years of the current climate of 1965–2015 and the future climate of 2050–2099, an inter-model consensus emerges, with a total of 34 out of 43 (79.1%) models under SSP585, and 27 out of 39 (69.2%) models under SSP126, generating an increase in Niño3.4 SST variability (Fig. 2a,b). Thus, as the period for calculating ENSO statistics lengthens, the influence of internal variability tapers off, whereas the effect of greenhouse warming is better diagnosed.

Studies based on CMIP5 models alone, or on a combination of CMIP5 and a smaller set of earlier available CMIP6 models[9,10], have found that models better simulating ENSO dynamics tend to generate increased ENSO SST variability. Nonlinear Bjerknes feedback is particularly important, in which once warm SST anomalies establish deep atmospheric convection in the equatorial eastern Pacific, the response of equatorial zonal wind anomalies increases nonlinearly to further sea surface warming[19], amplifying El Niño growth[10]. Models generally underestimate this feedback[10]. As a result, an inter-model consensus of increased ENSO SST variability emerges in a subset of models that simulate a reasonably realistic nonlinear positive feedback[10].

Under greenhouse warming, an increased air–sea coupling arising from an enhanced upper equatorial ocean stratification underpins the increase in ENSO variability[10]. There is a tendency for models that simulate stronger nonlinear Bjerknes feedback to generate a greater future increase in ENSO variability, and vice versa, and this relationship is statistically significant above the 99% confidence level (Extended Data Fig. 6). As such, the skewness in three model outliers that project a decrease in ENSO variability in Figs. 1 and 2 is either small (UKESM1-0-LL) or negative (BCC-CSM2-MR, CESM2). Besides some improvements in the representation of the tropical Pacific climate[20], more CMIP6 models simulate realistic ENSO nonlinear feedbacks[7]. The associated stronger air–sea coupling over the transient period of increasing greenhouse forcing

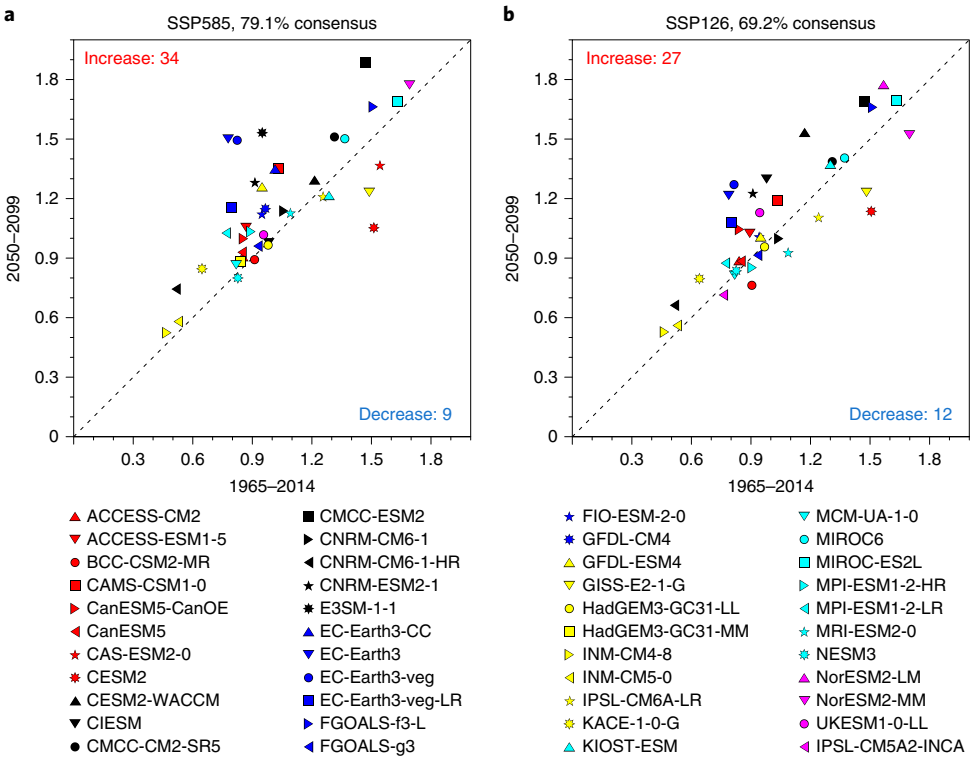


**Fig. 2 | Inter-model consensus on increased ENSO variability over a 50-year period. a,b**, ENSO Niño3.4 SST variability (in °C) in 50-year period of the current climate ending 2014 (*x* axis) and 50-year period of the future climate ending 2099 (*y* axis), under SSP585 (**a**) and SSP126 (**b**), respectively. The number of models generating an increase/decrease in ENSO variability is indicated in the top-left/bottom-right corner. Using the period length of 50 years sees a total of 34 out of 43 (79.1%) models under SSP585, and 27 out of 39 (69.2%) models under SSP126 produce increased ENSO SST variability.

probably contributes to the strong inter-model consensus even when all available models are used.

Putting our results in a broader context of recent studies, we note findings of decreased ENSO variability[21,22] in equilibrium state after an instantaneous doubling/quadrupling of $CO_2$, which seemingly contradict our conclusion; thus, it is worth highlighting that our result of increased ENSO SST variability is based on the IPCC 21st century 'transient' warming scenarios. Further, ocean mesoscale eddy-induced vertical heat transport is part of ENSO dynamics[22], but is not resolved in CMIP6 models; as such, whether or how incorporation of ocean mesoscale eddies alters our conclusion is not known. In addition, our conclusion is based solely on CMIP6 models, but a recent study based on 36 CMIP5 models and 20 CMIP6 models[23] finds a large spread in the projected ENSO change with no inter-model consensus; the discrepancy suggests a sensitivity of our result to model generations. We also note that our result is opposite to an observed decline in ENSO variability since 1999/2000 (ref. [24]); however, any greenhouse warming-induced ENSO variability change in the two decades since 1999/2000 might be masked by decadal variability and not yet detectable. Finally, the impact of North Pacific SST variability on ENSO is more realistically simulated in CMIP6 than in CMIP5, and the impact is enhanced under warmer background SSTs, contributing to enhanced future ENSO SST variability[25].

To conclude, in contrast to the IPCC AR6 assessment, there is in fact an inter-model consensus of increased ENSO SST variability in the 21st century from that of the 20th century under all four plausible SSP scenarios considered by the IPCC AR6 using CMIP6 models. The inter-model consensus is seen by comparing ENSO SST variability over the two 100-year periods of the 20th and 21st centuries. A long analysis period reduces the effect of internal variability, allowing a better detection of the greenhouse-forced effect. The increased inter-model consensus in CMIP6 is facilitated by improvements in the representation of ENSO processes, for example, nonlinear positive feedbacks, thus underscoring the importance of sustained model improvement in a multi-model approach toward reliable future projections. The inter-model consensus, particularly in the scenario with the strong mitigation pathway, highlights the need to consider the possibility of increased ENSO SST variability in addition to increased ENSO-induced rainfall variability.

## Online content

Any methods, additional references, Nature Research reporting summaries, source data, extended data, supplementary information, acknowledgements, peer review information; details of author contributions and competing interests; and statements of data and code availability are available at https://doi.org/10.1038/s41558-022-01282-z.

Received: 25 August 2021; Accepted: 6 January 2022;
Published online: 31 January 2022

## References

1. IPCC *Climate Change 2021: The Physical Science Basis* (eds Masson-Delmotte, V. et al.) (Cambridge Univ. Press, in the press).
2. Power, S. B., Delage, F., Chung, C., Kociuba, G. & Keay, K. Robust twenty-first century projections of El Niño and related precipitation variability. *Nature* **502**, 541–545 (2013).
3. Cai, W. et al. Increasing frequency of extreme El Niño events due to greenhouse warming. *Nat. Clim. Change* **4**, 111–116 (2014).
4. Wang, G. et al. Continued increase of extreme El Niño frequency long after 1.5 °C warming stabilization. *Nat. Clim. Change* **7**, 568–572 (2017).
5. Fredriksen, H.-B., Berner, J., Subramanian, A. C. & Capotondi, A. How does El Niño-Southern Oscillation change under global warming – a first look at CMIP6. *Geophys. Res. Lett.* **47**, e2020GL090640 (2020).

6. Yang, Y. et al. Greenhouse warming intensifies north tropical Atlantic climate variability. *Sci. Adv.* **7**, eabg9690 (2021).
7. Cai, W. et al. Changing El Niño–Southern Oscillation in a warming climate. *Nat. Rev. Earth Environ.* https://doi.org/10.1038/s43017-021-00199-z (2021).
8. Eyring, V. et al. Overview of the Coupled Model Intercomparison Project Phase 6 (CMIP6) experimental design and organization. *Geosci. Model Dev.* **9**, 1937–1958 (2016).
9. Cai, W. et al. ENSO and greenhouse warming. *Nat. Clim. Change* **5**, 849–859 (2015).
10. Cai, W. et al. Increased variability of eastern Pacific El Niño under greenhouse warming. *Nature* **564**, 201–206 (2018).
11. Ashok, K., Behera, S. K., Rao, S. A., Weng, H. Y. & Yamagata, T. El Niño Modoki and its possible teleconnection. *J. Geophys. Res.* **112**, C11007 (2007).
12. Cai, W. et al. Climate impacts of the El Niño–Southern Oscillation on South America. *Nat. Rev. Earth Environ.* **1**, 215–231 (2020).
13. Collins, M. et al. The impact of global warming on the tropical Pacific Ocean and El Niño. *Nat. Geosci.* **3**, 391–397 (2010).
14. Maher, N., Matei, D., Milinski, S. & Marotzke, J. ENSO change in climate projections: forced response or internal variability? *Geophys. Res. Lett.* **45**, 11–390 (2018).
15. Zheng, X.-T., Hui, C. & Yeh, S. W. Response of ENSO amplitude to global warming in CESM large ensemble: uncertainty due to internal variability. *Clim. Dyn.* **50**, 4019–4035 (2018).
16. Cai, W. et al. Butterfly effect and a self-modulating El Niño response to global warming. *Nature* **585**, 68–73 (2020).
17. Li, J. et al. Interdecadal modulation of El Niño amplitude during the past millennium. *Nat. Clim. Change* **1**, 114–118 (2011).
18. Austin, P. C. & Tu, J. V. Bootstrap methods for developing predictive models. *Am. Stat.* **58**, 131–137 (2004).
19. Dommenget, D., Bayr, T. & Frauen, C. Analysis of the non-linearity in the pattern and time evolution of El Niño–Southern Oscillation. *Clim. Dyn.* **40**, 2825–2847 (2013).
20. Planton, Y. et al. Evaluating climate models with the CLIVAR 2020 ENSO metrics package. *Bull. Am. Meteorol. Soc.* **102**, E193–E217 (2021).
21. Callahan, C. W. et al. Robust decrease in El Niño/Southern Oscillation amplitude under long-term warming. *Nat. Clim. Change* **11**, 752–757 (2021).
22. Wengel, C. et al. Future high-resolution El Niño/Southern Oscillation dynamics. *Nat. Clim. Change* **11**, 758–765 (2021).
23. Beobide-Arsuaga, G. et al. Uncertainty of ENSO-amplitude projections in CMIP5 and CMIP6 models. *Clim. Dyn.* **56**, 3875–3888 (2021).
24. Hu, Z.-Z. et al. The interdecadal shift of ENSO properties in 1999/2000: a review. *J. Climate* **33**, 4441–4462 (2020).
25. Jia, F. et al. Enhanced North Pacific impact on El Niño/Southern Oscillation under greenhouse warming. *Nat. Clim. Change* **11**, 840–847 (2021).

## Methods

**CMIP6 models.** Outputs were analysed for SST from all available CMIP6 under four emission scenarios (SSP126, SSP245, SSP370 and SSP585), each covering 200 years from 1900 to 2099 (Supplementary Table 1). SSP126 represents a strong mitigation pathway for achieving the warming target of the Paris Agreement. These models were forced under historical forcing up to 2014 and different emission scenarios thereafter[8]. For a given model, outputs might not be available for all emission scenarios; for example, outputs from 39 models were available under SSP126, whereas outputs from 43 models were available under SSP585.

We used one experiment from each model. Monthly climatology was constructed over the 1900–1999 period, and monthly SST anomalies referenced to the climatology were obtained. Time series of the 200-year SST anomalies averaged over regions of ENSO SST indices, Niño3 (5° N–5° S, 150° W–90° W), Niño4 (5° N–5° S, 160° E–150° W) and Niño3.4 (5° N–5° S, 170° W–120° W) was quadratically detrended over the full 200-year period. We compared the standard deviation of an ENSO SST index over two periods, either between the 2000–2099 and 1900–1999 (Fig. 1), or between the 50-year future climate of 2050–2099 and current climate of 1965–2014 (Fig. 2).

**Bootstrap test.** A bootstrap method[18] was used to examine whether the multi-model mean increase in variability of an ENSO SST index is statistically significant. For example, under SSP585, the 43 values of Niño3.4 SST variability in the 20th century were resampled randomly to form 10,000 realizations of 43-sampled sets. A histogram of the 10,000 realizations (blue bars), together with the 10,000 inter-realization standard deviation (grey shade), is shown in Extended Data Fig. 1. The same process was repeated for the 21st century. If the increased multi-model mean in Niño3.4 SST variability is greater than variability due to internal variability, that is, the sum of the 10,000 inter-realization standard deviation values for the 20th and 21st centuries, the increase is statistically significant above the 95% confidence level. Because ENSO SST variability varies vastly across models (Fig. 1), an alternative approach is to have an ENSO SST index in each model normalized by the standard deviation over the full 200-year period before conducting the multi-model average and the Bootstrap test. In this approach, the statistical significance holds (Extended Data Fig. 2).

## Data availability

Data related to the paper can be downloaded from websites listed below: CMIP6 database, https://esgf-node.llnl.gov/projects/cmip6/. Detailed references and DOI URLs for each CMIP6 model are provided in Supplementary Information.

## Code availability

Codes for calculating ENSO SST variability are available from the corresponding authors on request.

## References

26. Rayner, N. A. A. et al. Global analyses of sea surface temperature, sea ice, and night marine air temperature since the late nineteenth century. *J. Geophys. Res. Atmos.* **108**, 4407 (2003).

## Acknowledgements

This project was supported by the Strategic Priority Research Program of the Chinese Academy of Sciences, grant number XDB40030000. L.W. was supported by the National Key Research and Development Program of China (2019YFC1509100). W.C., B.N., G.W. and A.S. were supported by CSHOR. CSHOR is a joint research Centre for Southern Hemisphere Oceans Research between QNLM and CSIRO. W.C., B.N., G.W. and A.S. were also supported with funding from the Australian Government under the National Environmental Science Program (NESP). The funders had no role in study design, data collection and analysis, decision to publish or preparation of the manuscript. We thank J. Fyfe for helpful discussion on the AR6 assessment; the World Climate Research Programme, which, through its Working Group on Coupled Modelling, coordinated and promoted CMIP6; the climate modelling groups for producing and making available their model output; the Earth System Grid Federation (ESGF) for archiving the data and providing access; and the multiple funding agencies that supported CMIP6 and ESGF.

## Author contributions

W.C. wrote the initial manuscript; B.N. conducted the analysis in discussion with W.C. and G.W.; A.S., L.W. and K.Y. contributed to interpreting results and improvement of this paper.

## Competing interests

The authors declare no competing interests.

## Additional information

**Extended data** is available for this paper at https://doi.org/10.1038/s41558-022-01282-z.

**Supplementary information** The online version contains supplementary material available at https://doi.org/10.1038/s41558-022-01282-z.

**Correspondence and requests for materials** should be addressed to Wenju Cai or Lixin Wu.

**Peer review information** *Nature Climate Change* thanks Zeng-Zhen Hu and the other, anonymous, reviewer(s) for their contribution to the peer review of this work.

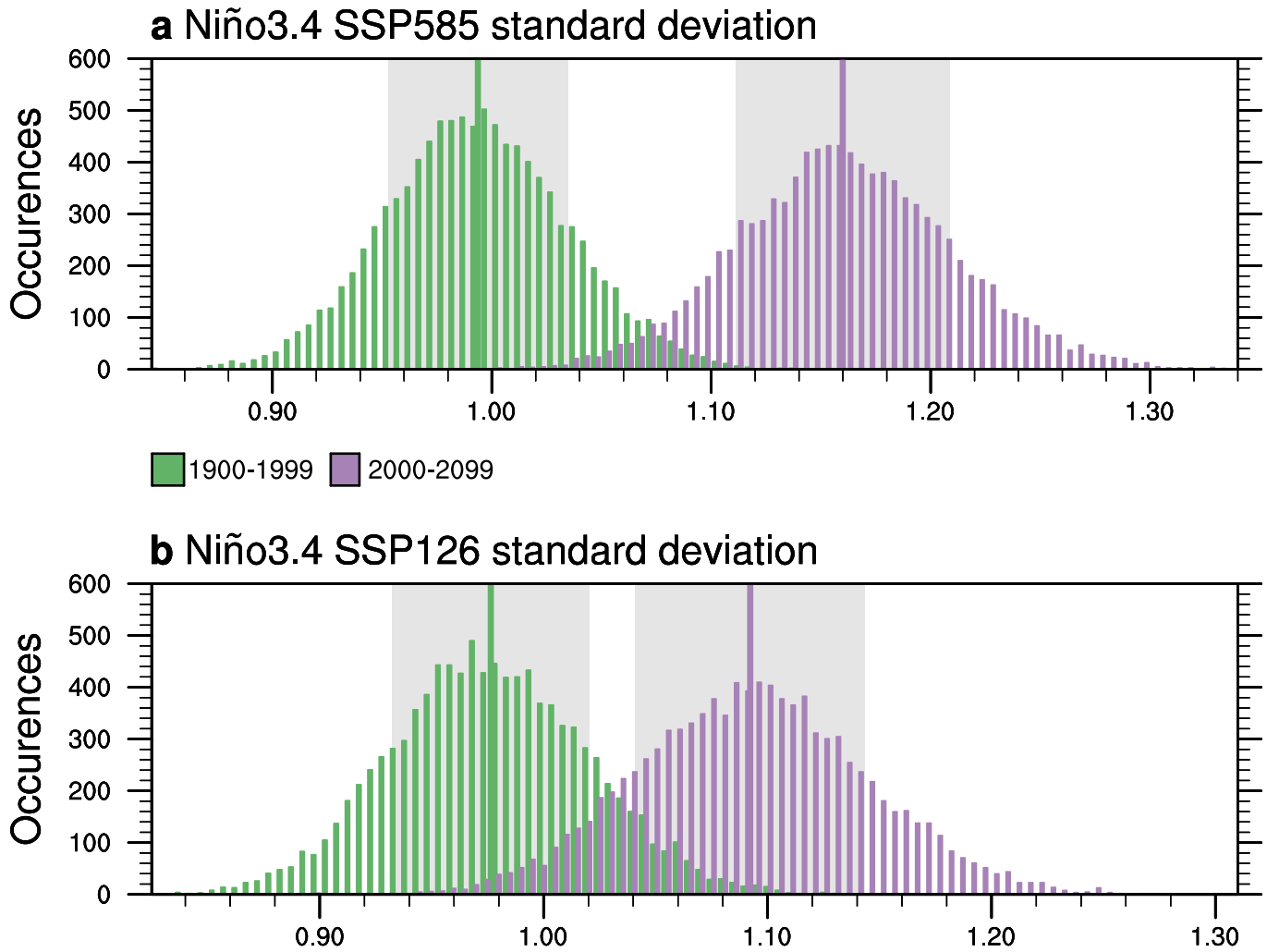


**Extended Data Fig. 1 | Illustration of statistical significance of multi-model ensemble mean change.** Uncertainty in the multimodel mean is calculated as 1.0 s.d. of the 10,000 inter-realizations of a bootstrap method (see 'Bootstrap test' section in Methods), for **a** the SSP585, and **b** the SSP126 emission scenario. The green and purple vertical lines indicate the mean values of 10,000 inter-realizations for the 20$^{th}$ and 21$^{st}$ century, respectively, identical to the multi-model ensemble means shown Fig. 1. The grey shaded regions indicate the respective 1.0 s.d. of the 10,000 inter-realization.

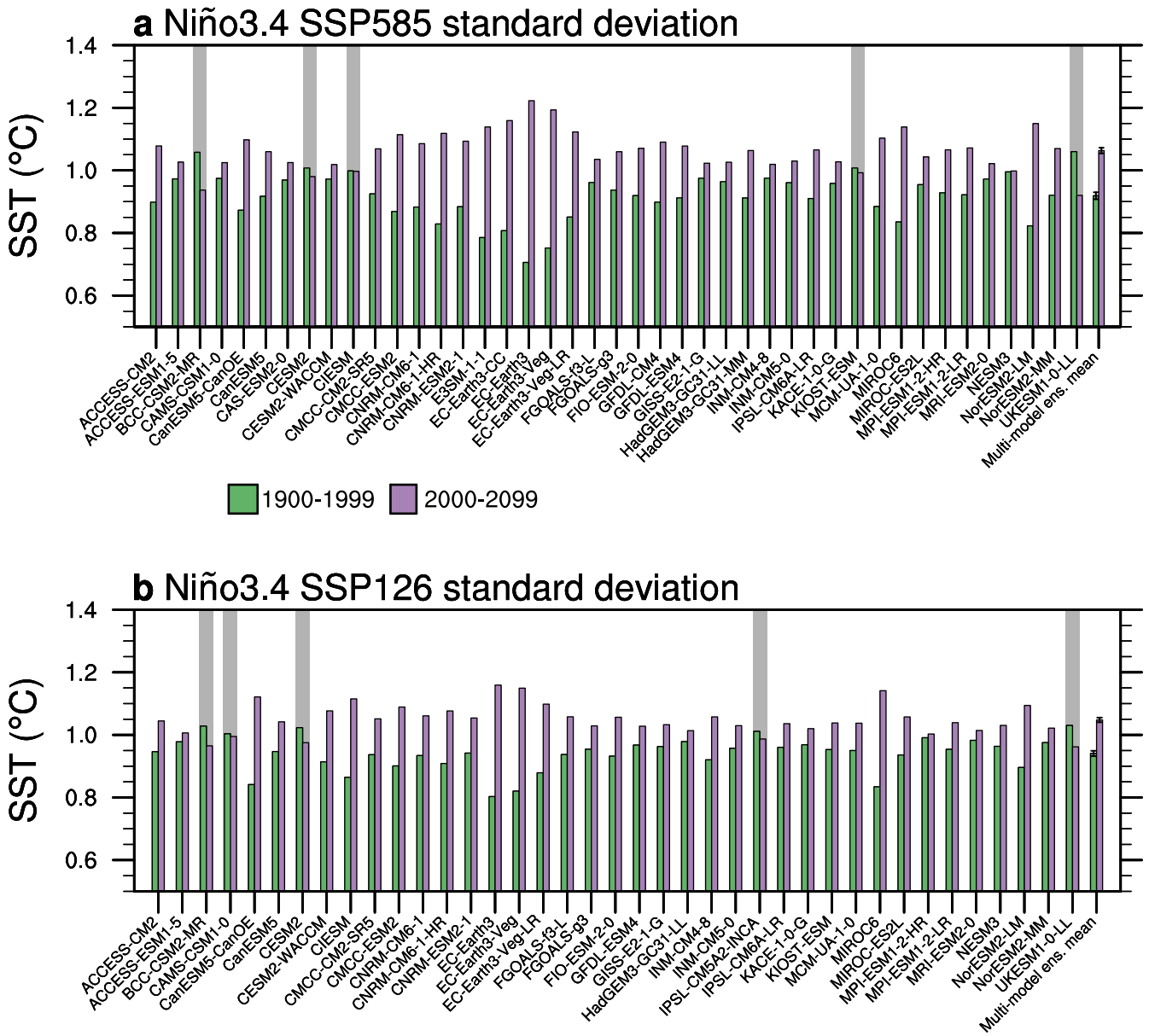


**Extended Data Fig. 2 | An inter-model consensus on increased ENSO SST variability.** The same as in Fig. 1, except in each model the ENSO SST index is normalized by the standard deviation (s.d.) over the whole 200 years. ENSO Niño3.4 SST variability (s.d.) over the 20th century (1900–1999, green bars) and the 21st century (2000–2099, purple bars), from **a** 43 available CMIP6 models under the SSP585 scenario, and **b** 39 CMIP6 models under the SSP126 scenario, with an 88.4% and 87.2% of models showing an increase in ENSO variability. The grey shading indicates models which do not simulate an increase. Also shown is the multi-model ensemble mean for each period. The range in the multi-model mean bars is defined as the value of standard deviation of inter-model variability in the 20th and 20st century, respectively, determined by a Bootstrap test (see 'Bootstrap test' in Methods). The difference in the multi-model mean is statistically significant above the 95% confidence level.

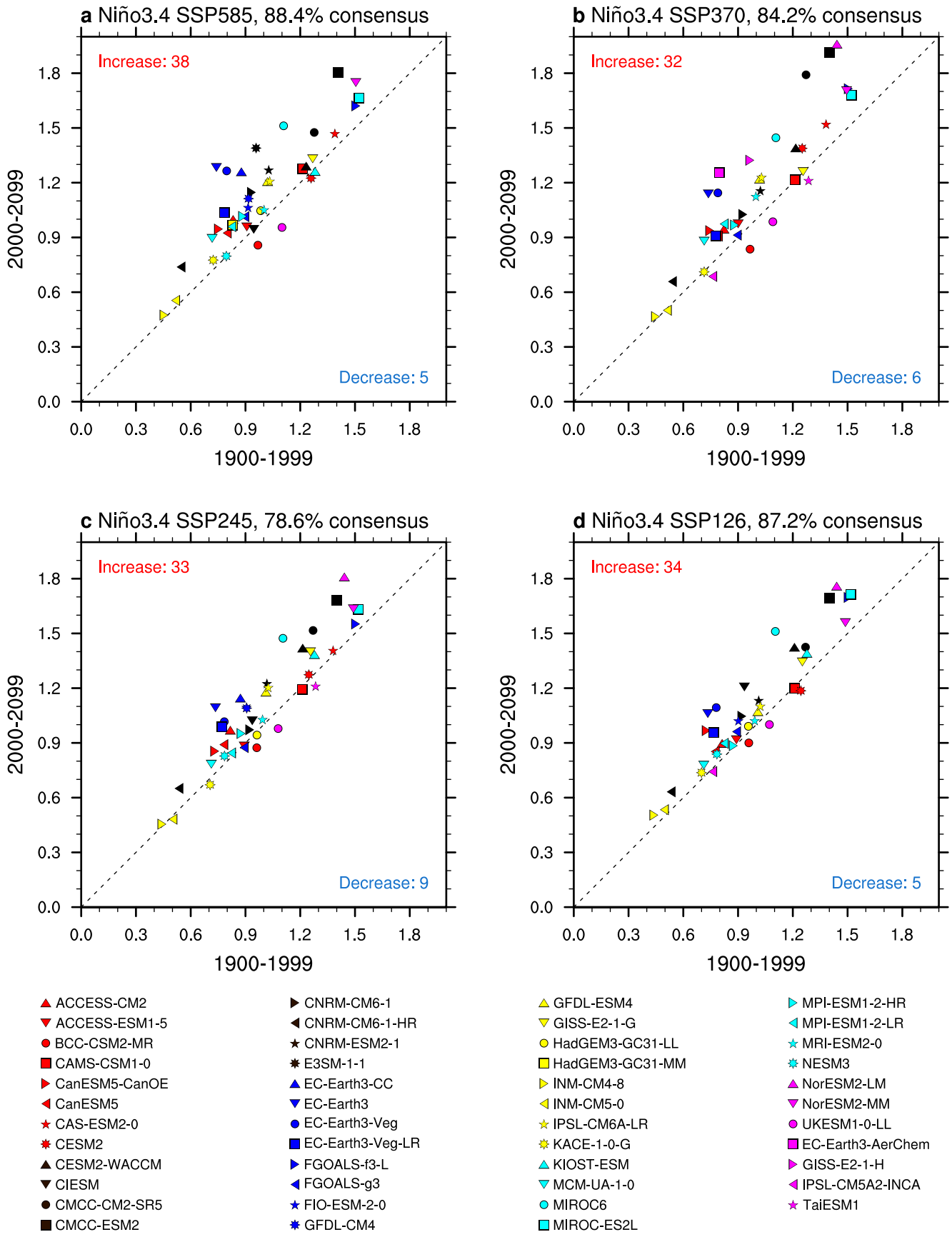


**Extended Data Fig. 3 | Inter-model consensus on increased ENSO Niño3.4 variability in 21st century. a–d**, ENSO Niño3.4 SST variability (in °C) in the 20th century climate (x-axis) and the 21st century climate (y-axis), under the SSP585, SSP370, SSP245, and SSP126 emission scenarios, respectively. The number of models generating an increase in ENSO variability is indicated in the top-left corner, and number of models producing a decrease in ENSO variability is indicated in the bottom right corner. The inter-model consensus range is 78.6–88.4%.

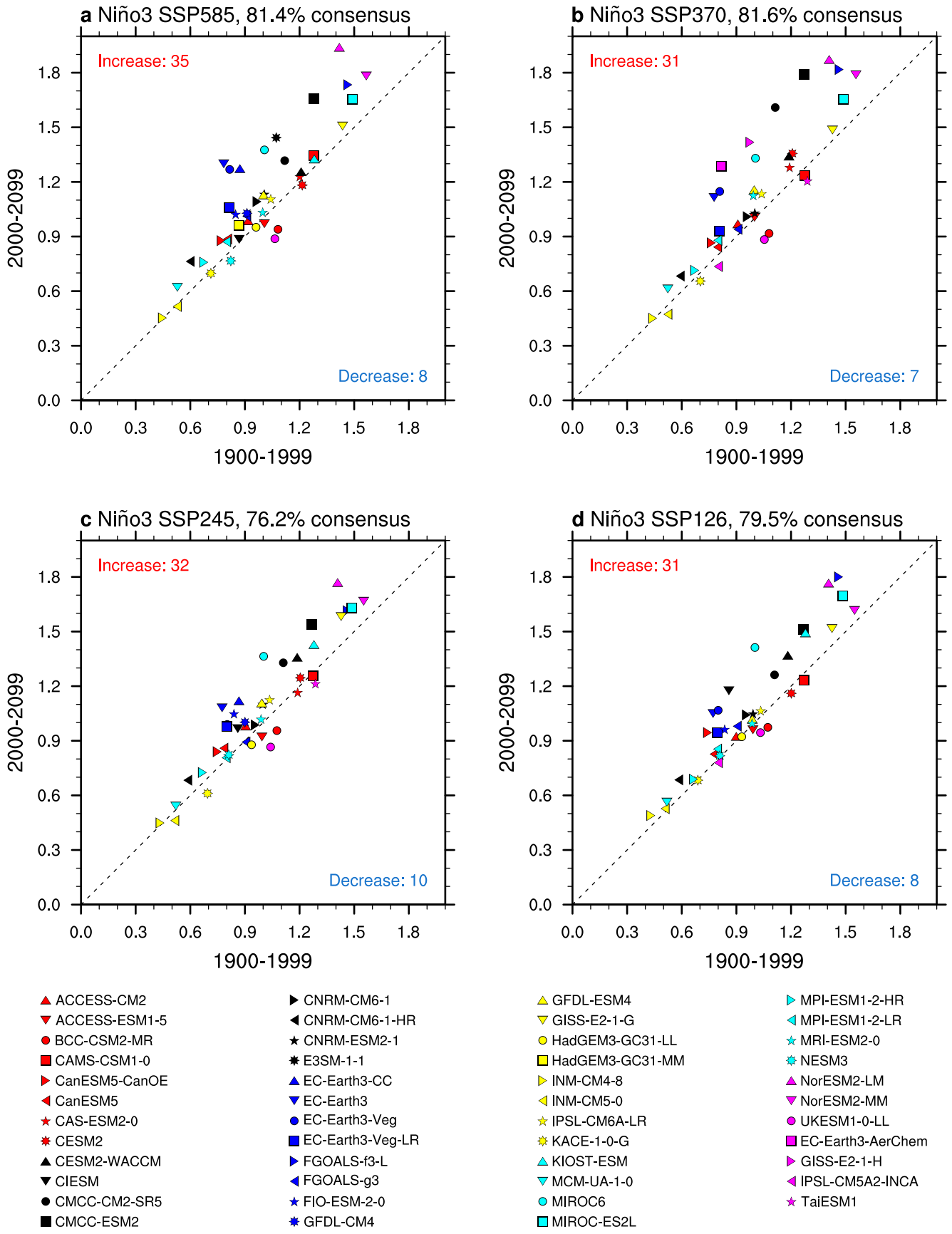


**Extended Data Fig. 4 | Inter-model consensus on increased ENSO Niño3 variability in 21st century. a–d**, ENSO Niño3 SST variability (in °C) in the 20th century (x-axis) and the 21st century (y-axis), under the SSP585, SSP370, SSP245, and SSP126 emission scenarios, respectively. The number of models generating an increase in ENSO variability is indicated in the top-left corner, and number of models producing a decrease in ENSO variability is indicated in the bottom right corner. The inter-model consensus range is 76.2–81.6%.

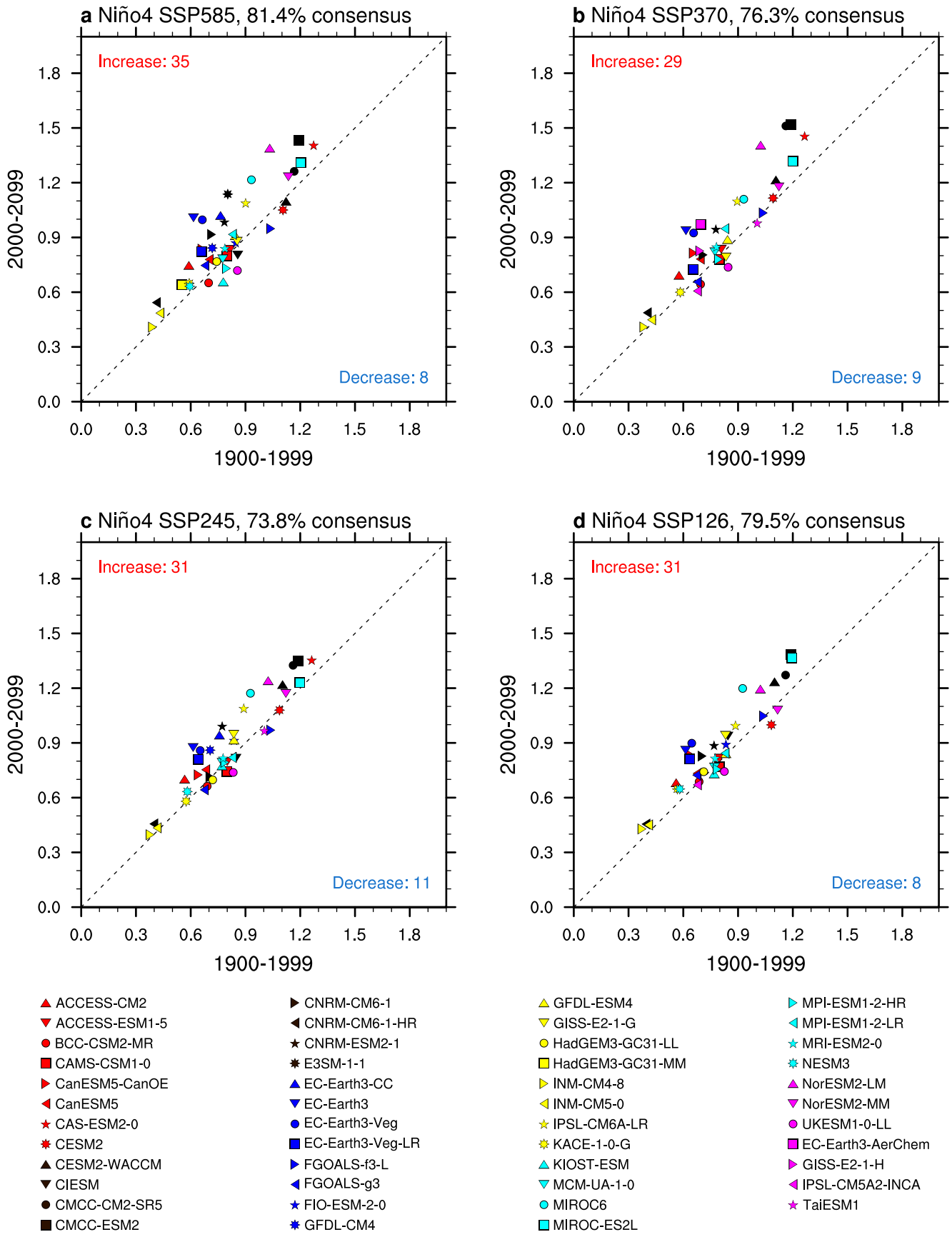


**Extended Data Fig. 5 | Inter-model consensus on increased ENSO Niño4 variability in 21st century. a–d**, ENSO Niño4 SST variability (in °C) in the 20th century climate (x-axis) and the 21st century (y-axis), under the SSP585, SSP370, SSP245, and SSP126 emission scenarios, respectively. The number of models generating an increase in ENSO variability is indicated in the top-left corner, and number of models producing a decrease in ENSO variability is indicated in the bottom right corner. The inter-model consensus range is 73.8–81.4%.

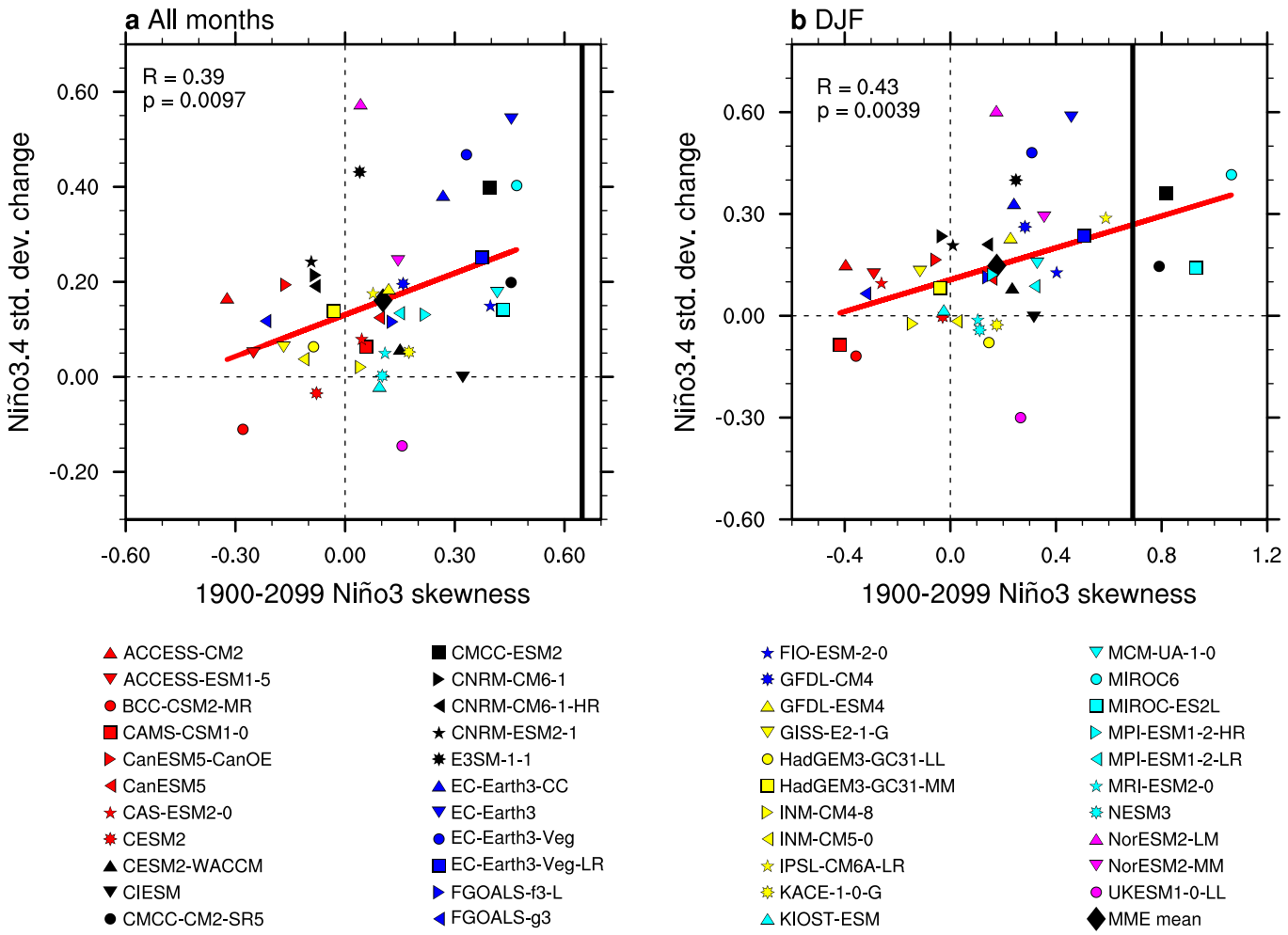


**Extended Data Fig. 6 | 21st century Niño3.4 variability change (°C) and nonlinear Bjerknes feedback represented by Niño3 SST skewness.** Shown are for the SSP585 emission scenario, **a**, based on monthly value, and **b**, based on ENSO peak season of December, January, and February (DJF). Observed skewness based on 1900–2020 from a reanalysis[26] is shown as a black solid vertical line in each panel. Correlation coefficient and the *P*-value are shown in each panel, indicating statistically significant relationships above the 99% significance level. SST skewness in the eastern equatorial Pacific is an integral component of a parameter that also encapsulates skewness in the central Pacific to depict ENSO nonlinearity as a whole[7,10]. In terms of this nonlinearity parameter, a larger number of CMIP6 (79%) than CMIP5 (55%) models simulate greater than one third of the observed parameter.